(7) Elemental analyses performed by Midwest Microlabs. Anal. Calcd for $Rb_2[Pt(CN)_4](FHF)_{0.40}$: C, 9.89; N, 11.54; H, 0.08; F, 3.13. Found: C, 9.66; N, 10.53; H, 0.15; F, 3.05, 3.15. Emission spectrographic analyses for metal content performed by J. P. Faris indicated only Rb and Pt were present.
(8) H. L. Carell and J. Donohue, *Isr. J. Chem.*, **10**, 195 (1972).
(9) D. Cahen, *Solid State Commun.*, **12**, 1091 (1973).
(10) L. Pauling, "The Nature of the Chemical Bond", 3rd ed, Cornell University Press, Ithaca, N.Y., 1960, pp 398–404.
(11) J. M. Williams, *Inorg. Nucl. Chem. Lett.*, **12**, 651 (1976).
(12) A. H. Reis, Jr., and S. W. Peterson, *Inorg. Chem.*, **15**, 3186 (1976).
(13) T. W. Thomas, C. Hsu, M. M. Labes, P. S. Gomm, A. E. Underhill, and D. M. Watkins, *J. Chem. Soc., Dalton Trans.*, 2050 (1972); C. Jacobsen, K. Carneiro, and J. M. Williams, work in progress.

Contribution from the Instituto de Optica "Daza de Valdés", C.S.I.C., Serrano, 121 Madrid-6, Spain

A Model for B Carbonate Apatite

M. Santos* and P. F. González-Díaz

Received January 26, 1977 AIC700695

Although the mechanism of substitution of CO_3^{2-} ions and the precise site these ions occupy in the lattice of A carbonate apatite are well established,[1] neither a complete mechanism of CO_3^{2-} substitution nor the exact site these ions occupy in the lattice of B carbonate apatite has hitherto been determined.[2] Nevertheless, it is known[3] that the *c* axis of the unit cell of B carbonate apatite and the perpendicular to the CO_3^{2-} plane form an angle of around 35°.

Bonel et al.[4] have determined the Ca^{2+}/PO_4^{3-}, Ca^{2+}/CO_3^{2-}, and Ca^{2+}/OH^- ratios in a great number of synthetic B carbonate apatites and proposed the general formula to account for these compounds

$$Ca_{10-x+u}(PO_4)_{6-x}(CO_3)_x(OH)_{2-x+2u}(H_2O)_z$$
1

where $0 \le x \le 2$, $0 \le u \le x/2$, and z is an unlimited variable. Since the substitution of a PO_4^{3-} ion by a CO_3^{2-} ion should leave a negative residual electric charge in the unit cell, Bonel et al. assumed that a couple, OH^- and Ca^{2+}, is removed away from the apatitic lattice in each PO_4^{3-}–CO_3^{2-} interchange, so that the number of Ca^{2+} and OH^- per unit cell decreases when substitution increases. Further, the *u* and *z* parameters in formula **1** are introduced to account only for the experimental values of the Ca^{2+}/PO_4^{3-}, Ca^{2+}/CO_3^{2-}, and Ca^{2+}/OH^- ratios.

Experimental Section

Stoichiometric and nonstoichiometric hydroxylapatite were prepared by a modified method of Winand.[5] A–B carbonate apatite was synthesized by a similar procedure in which sodium carbonate was added to the initial solution of Na_2HPO_4. B carbonate apatite was obtained by heating at 900 °C for 1 h a mixture of A–B carbonate apatite with calcium fluoride in a current of 2 cm^3/s of dry CO_2. This reaction was carried out in a tube inserted in a furnace.

Biological carbonate apatites were provided by Dr. L. Cifuentes of the Urolithiasis Laboratory, Fundacion Jimenez Diaz, Madrid.

The x-ray diffraction pattern, electron microscopy, and electron diffraction diagram do not detect the presence of specimens such as $CaCO_3$, $CaHPO_4$, etc. in all of the samples so that these are practically constituted by single-phased nonstoichiometric carbonate apatites.

Infrared absorption spectra were recorded on a Perkin-Elmer 457 spectrophotometer in the range 4000–250 cm^{-1}. Absorption cells were prepared using the KBr disk technique.

Results and Discussions

Figure 1 shows the mid-IR spectrum of a synthetic A–B carbonate apatite. CO_3^{2-} bands in this spectrum appear at 1542, 1462, 1412, 880, and 872 cm^{-1}, which indicates that the two types of substitution (A and B) are present in this compound.

Figure 2 shows the mid-IR spectrum of the above sample heated at 900 °C for 3 h. In this spectrum, nearly stoichiometric hydroxylapatite $Ca_{10}(PO_4)_6(OH)_2$[5] and calcium hydroxide are seen; it can also be observed that some amount of the CO_3^{2-} ions still remain inside the apatitic structure.

Since in the present conditions calcium hydroxide can only originate from calcium carbonate, it is not possible to postulate a general thermal mechanism by which formula **1** gives rise to the compound appearing in the IR spectrum of Figure 2. Moreover, as evidenced by this spectrum, the amount of CO_3^{2-} ions included in the apatitic lattice is very small after calcination; therefore, some proportion of the stoichiometric hydroxylapatite observed in the spectrum of Figure 2 has to originate from the initial B carbonate apatite. This fact also cannot be explained by the formula assumed by Bonel et al.

Figure 3 reports the mid-IR spectrum of a B carbonate apatite. The CO_3^{2-} IR bands appear at 1450, 1425, and 862 cm^{-1}. Figure 4 gives the mid-IR spectrum of the same sample after calcination at 900 °C. Besides the presence of some small proportion of CO_3^{2-} ions included in the apatitic lattice, this spectrum corresponds to that of fluoroapatite, which confirms the above assessments.

A–B carbonate apatite might be obtained by CO_3^{2-} diffusion through a suspension of nonstoichiometric hydroxylapatite.[6] However no carbonate apatite of any kind is formed in this process when stoichiometric hydroxylapatite is used.

Nonstoichiometric hydroxylapatite, $Ca_{10-x}(PO_4)_{6-x}(HPO_4)_x(OH)_{2-x}\cdot xH_2O$, differs from stoichiometric hydroxylapatite by possessing certain proportions of HPO_4^{2-} ions and water molecules. Therefore, HPO_4^{2-} ions and/or water molecules have to be responsible for the formation of carbonate apatites.

If we assume that CO_3^{2-} ions substitute for HPO_4^{2-} ions in nonstoichiometric hydroxylapatite, as the preceding synthetic procedure seems to indicate, the resulting compound would be electrically compensated.

$$Ca_{10-x}(PO_4)_{6-x}(CO_3)_x(OH)_{2-x}\cdot xH_2O$$
2

We have considered that the substitution of HPO_4^{2-} by CO_3^{2-} is complete. This does not modify the qualitative meaning of the arguments that hereafter will be presented.

Rotation of water molecules around the *c* axis in the unit cell of nonstoichiometric hydroxylapatite gives rise[7] to the alternative formation of the $[2PO_4^{3-}, OH^-, HPO_4^{2-}]$ and $[3PO_4^{3-}, H_2O]$ grouping through internal hydrogen migrations. When averaged over all possible water rotations in the crystal, the number of HPO_4^{2-} ions and water molecules become the same in a dynamical equilibrium. Such an equilibrium is broken in formula **2**, so that the internal system, H_2O, OH^-, PO_4^{3-}, of the hypothetical compound represented by formula **2** has to evolve in order to recover the dynamical equilibrium between the HPO_4^{2-} ions and the water molecules. Thus, formula **2** becomes

$$Ca_{10-x}(PO_4)_{6-3x/2}(CO_3)_x(HPO_4)_{x/2}(OH)_{2-x/2}\cdot(x/2)H_2O$$
3

Then, since the compound given by formula **3** has HPO_4^{2-} ions, new substitutions may occur, giving

$$Ca_{10-x}(PO_4)_{6-3x/2}(CO_3)_{3x/2}(OH)_{2-x/2}\cdot(x/2)H_2O$$
4

where we have again assumed that all HPO_4^{2-} have been substituted for by CO_3^{2-} ions. Considerations made on formula **2** apply again to formula **4**; therefore, new HPO_4^{2-} ions will be formed from water molecules. However these new HPO_4^{2-} ions cannot now be substituted for by CO_3^{2-} ions. In fact, CO_3^{2-} ions have to be bonded to Ca^{2+} ions, so the compound given by **4** must be considered to be a special mixture of

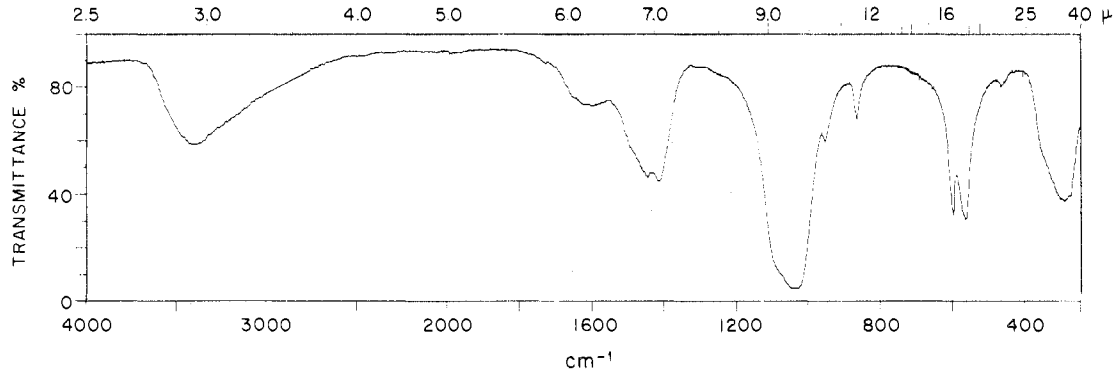

Figure 1. Mid-IR spectrum of a synthetic A–B carbonate apatite.

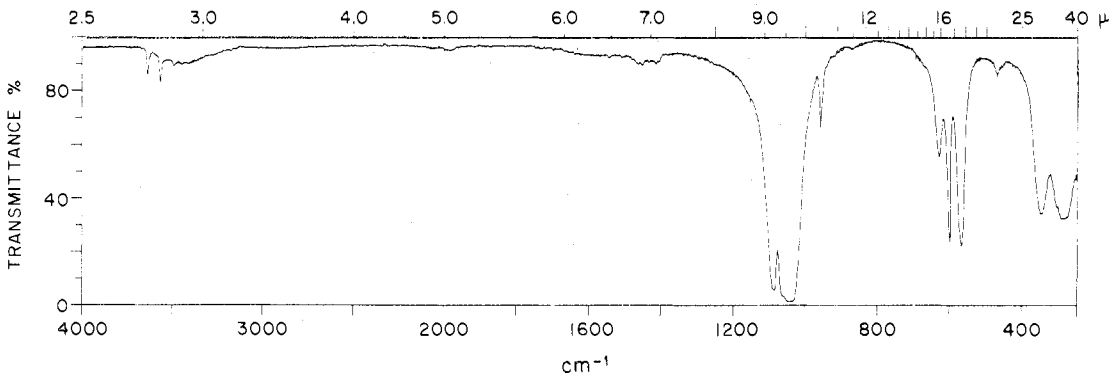

Figure 2. Mid-IR spectrum of a synthetic A–B carbonate apatite heated at 900 °C for 3 h.

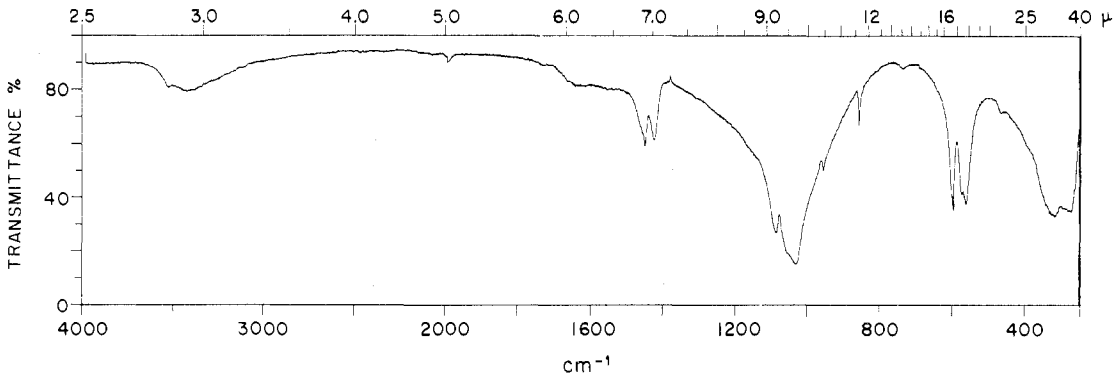

Figure 3. Mid-IR spectrum of a B carbonate apatite.

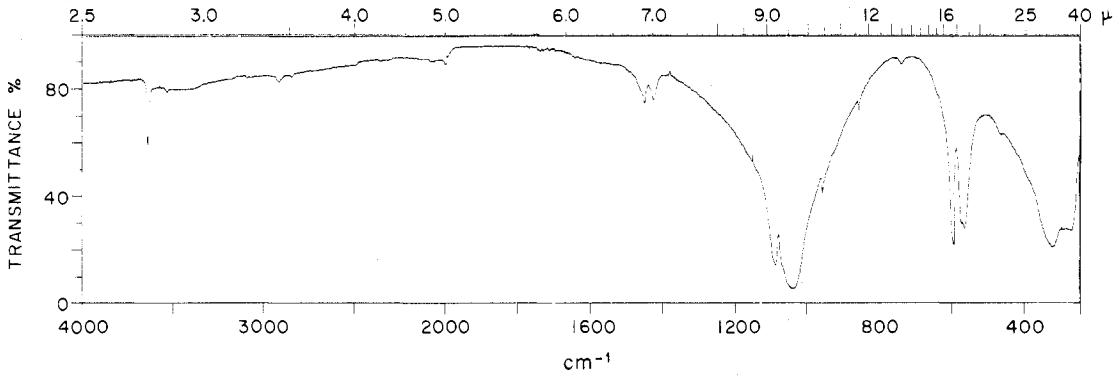

Figure 4. Mid-IR spectrum of a B carbonate apatite heated at 800 °C for 3 h.

calcium carbonate, hydroxylapatite, and water in the form

$$Ca_{10-5x/2}(PO_4)_{6-3x/2}(OH)_{2-x/2}\cdot(3x/2)CaCO_3\cdot(x/2)H_2O$$

5

since the apatitic part of mixture **5** has a Ca/P ratio of 1.66 and a Ca/OH ratio of 5, additional substitution of HPO_4^{2-} ions by CO_3^{2-} ions would give rise to special mixtures whose apatitic components should show Ca/OH and Ca/P ratios outside the range corresponding to the apatitic compounds. In this way, the final formula representing the B carbonate apatite when the substitution of HPO_4^{2-} by CO_3^{2-} is maximum becomes

$$Ca_{10-x}(PO_4)_{6-5x/4}(CO_3)_{3x/2}(HPO_4)_{x/4}(OH)_{2-x/4}\cdot(x/4)H_2O$$

6

However, CO_3^{2-} ions are located at the same sites as HPO_4^{2-}

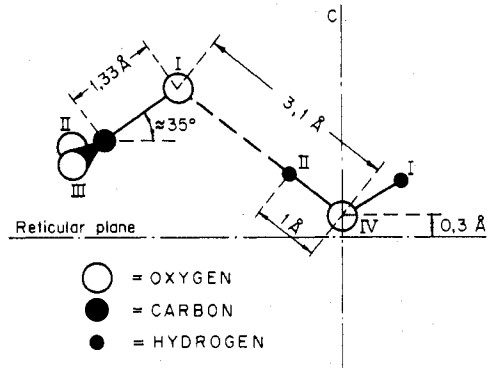

Figure 5. Relative positions of the water molecule and CO_3^{2-} ions in B carbonate apatite.

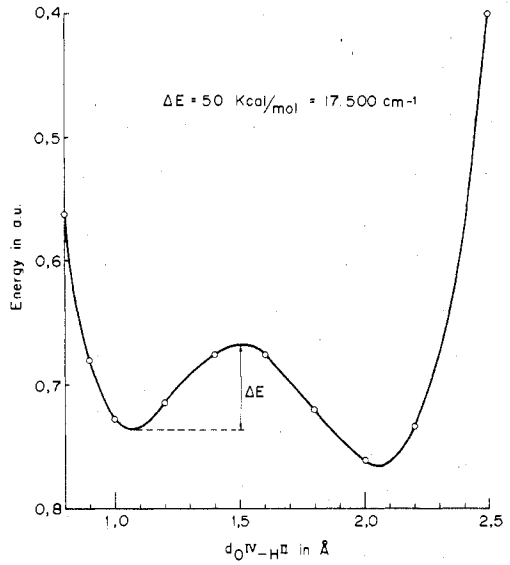

Figure 6. Potential function curve for the hydrogen motion along the $O^{IV}\cdots O^{I}$ line in Figure 5.

ions. As a consequence, one of the oxygens of CO_3^{2-} is in such a position that a hydrogen bond to this oxygen atom from the nearest OH group could be formed. Therefore, CO_3^{2-} ions may participate in the hydrogen migration mechanism described above; if so, some proportion of HCO_3^- ions has to appear and there would be no reason for postulating formula **6** as a good representation of B carbonate apatite.

The relative positions of the water molecule and CO_3^{2-} ions are given in Figure 5. Optimization of the H^{II} position in this figure, along the $O^{I}\cdots O^{IV}$ line, has been made using the CNDO/2 method.[8] Figure 6 shows the potential function curve corresponding to the different positions in which H^{II} is situated along the $O^{I}\cdots O^{IV}$ line. Two minima at 1.05 and 2.05 Å are observed in this curve; the first one corresponds to the $CO_3^{2-}\cdots H_2O$ configuration I whereas the second one corresponds to the $HCO_3^-\cdots OH^-$ configuration II. Since the energy of activation, ΔE, for passing from configuration I to configuration II is too large ($\sim$17 500 cm^{-1}), it would seem that the dynamical formation of the HCO_3^{2-} ions is forbidden in B carbonate apatite.

According to formula **6** the CO_3^{2-} content in B carbonate apatite may vary between 0 and $3x/2$ for a given value of the degree of nonstoichiometry x. The highest possible CO_3^{2-} content will occur in the octacalcium phosphate ($x = 2$) where the proportion of CO_3^{2-} may in principle vary between 0 and 3. For stoichiometric hydroxylapatite substitution of CO_3^{2-} is obviously impossible.

The proportion of hydrogen migrations per unit cell is expected to increase when the value of x increases from 0 to

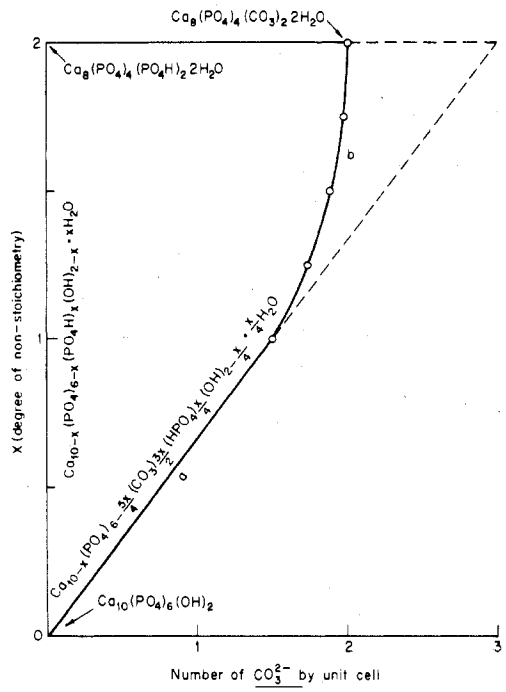

Figure 7. Domain for the set of B carbonate apatite.

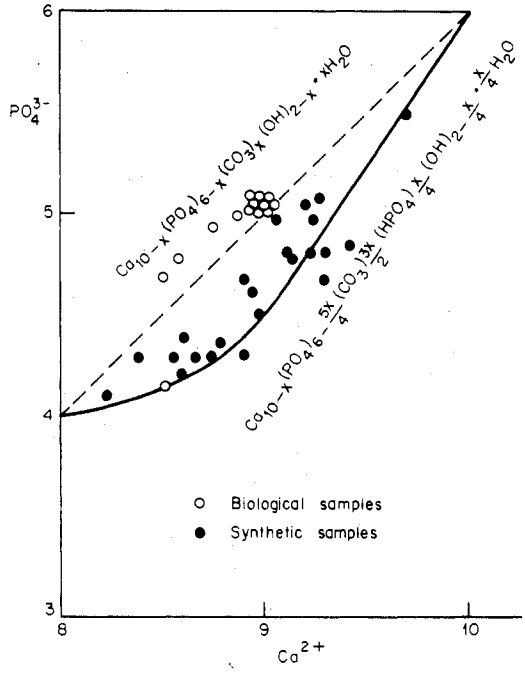

Figure 8. Theoretical domain for the Ca^{2+}/PO_4^{3-} ratio and values obtained in synthetic and biological samples.

1. However this proportion decreases when the value of x increases from 1 to 2, in such a way that no hydrogen migration is allowed for $x = 2$. In fact, the number of the $2PO_4^{3-}$, HPO_4^{2-}, H_2O configurations, in which no apparent migrations occur, increases from $x = 1$ to $x = 2$; then if the HPO_4^{2-} of each of these configurations is replaced by one CO_3^{2-} ion, there exists no possibility of further HPO_4^{2-} formation and, therefore, no new CO_3^{2-} may enter in the B sites. As a result, the range of CO_3^{2-} content per unit cell in octacalcium phosphate is reduced to run from 0 to 2.

The ruled area of Figure 7 represents the set of all the B carbonate apatites possible as predicted by our model. The specimens on lines a and b have the maximum of CO_3^{2-} substitutions. Line b is not straight because the second generation of HPO_4^{2-}–CO_3^{2-} interchanges is successively

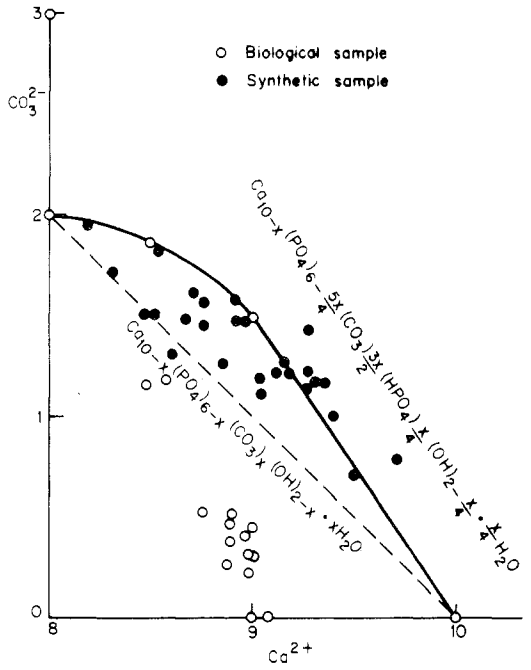

Figure 9. Theoretical domain for the Ca^{2+}/CO_3^{2-} ratio and values obtained in synthetic and biological samples.

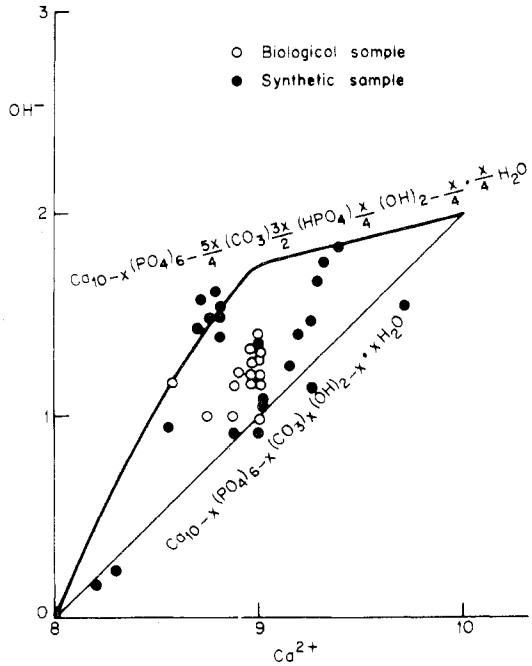

Figure 10. Theoretical domain for the Ca^{2+}/OH^- ratio and values obtained in synthetic and biological samples.

precluded when the value of x increases from 1 to 2.

The theoretical domain of the Ca^{2+}/PO_4^{3-}, Ca^{2+}/CO_3^{2-}, and Ca^{2+}/OH^- ratios predicted by our model are shown in Figures 8–10. The experimental values of these ratios for synthetic[4] and biological carbonate apatites are also shown on these figures. It can be observed that experimental values are collected by an enclosing curve as Bonel et al. reported.[4] For the case of biological carbonate apatites the Ca^{2+}/PO_4^{3-} and Ca^{2+}/CO_3^{2-} ratios occupy different regions inside the same domains. This fact can be explained because synthetic samples are formed in CO_3^{2-}-saturated media and, therefore, at least the first generation of CO_3^{2-} substitutions has to take place. This is not the case for biological samples whose characteristic ratios cannot be included in the representation given by Bonel et al.

Acknowledgment. The authors are indebted to Dr. L. Cifuentes of the Urolithiasis Laboratory, Fundación Jiménez Díaz, Madrid, for providing us with the biological carbonate apatites.

Registry No. Carbonate apatite, 12286-89-4.

References and Notes

(1) P. F. González-Díaz and A. Hidalgo, *Opt. Pur. Apl.*, **8**, 51 (1975).
(2) R. Z. Legeros, Ph.D. Thesis, New York University, 1967.
(3) J. C. Elliot, Ph.D. Thesis, London, 1964.
(4) G. Bonel, J. C. Labarthe, and C. Vignoles, "Physico-chimie et Cristallographie des apatites d'interet biologique, Paris, 10–15 September 1973", Editions du Centre National de la Recherche Scientifique, Paris, 1975.
(5) P. F. González-Díaz and A. Hidalgo, *Spectrochim. Acta, Part A*, **32**, 631 (1976).
(6) P. F. González-Díaz, Ph.D. Thesis, University of Complutense, Madrid, 1974.
(7) A. Hidalgo and P. F. González-Díaz, *C. R. Hebd. Seances Acad. Sci., Ser. B*, **280**, 563 (1975).
(8) J. A. Pople, G. A. Segal, and D. P. Santry, *J. Chem. Phys.*, **43**, S136, S129 (1965).

Contribution from the Departments of Chemistry, University of Karlsruhe, 75 Karlsruhe, West Germany, and Ames Laboratory—ERDA, Iowa State University, Ames, Iowa 50011

Rare Earth Metal–Metal Halide Systems. 19. Structural Characterization of the Reduced Holmium Chloride Ho_5Cl_{11}

U. Löchner,[1a] H. Bärnighausen,*[1a] and J. D. Corbett[1b]

Received January 26, 1977 AIC70068C

In recent years numerous rare earth metal–metal halide phase diagrams have been investigated, many of which contain one or more intermediate phases between the trihalide and the pure dihalide.[2] Once the structures of the salt-like dihalides became well understood,[3,4] gradually more insight has been gained into the structures of the intermediate phases in these systems.[5,6] In 1975 the condensed holmium–holmium(III) chloride system[2b] was described which featured a single reduced phase of analytical composition $HoCl_{2.14}$, the very narrow range between its peritectic melting point at 551 °C and the eutectic (with $HoCl_3$) at 543 °C contributing to the difficulty of the preparation. In the course of subsequent single crystal work on reduced rare earth halides, especially on Dy_5Cl_{11},[5] the holmium phase has now been structurally identified as the isostructural Ho_5Cl_{11}, that is, with the correct composition $HoCl_{2.20}$.

Experimental Section

The work utilized powder diffraction data secured photographically on an IRDAB (Stockholm) Guinier camera of 100 mm diameter with monochromatized Cu $K\alpha_1$ radiation, λ 1.540 562 Å. The diffraction intensities were measured on a Zeiss-Jena Schnellphotometer G III. Intensity readings from a scale $S = \log 1/D$ from 0 to ∞ were corrected for individual background, and the lightest background was set to zero and the primary beam line intensity to ∞. I_o values given in Table I (supplementary material) are photometer readings scaled to I_c.

Results and Discussion

The reduced holmium phase has the composition Ho_5Cl_{11} and is isomorphous with the monoclinic Dy_5Cl_{11}. The structure was identified using powder Guinier photographs collected during the original phase diagram work.[2b] As shown in Table I, 75 observed lines in the diffraction pattern can now be completely indexed with good agreement between observed and calculated[7] intensities. From these, 29 sharp and clearly resolved reflections were chosen for the final lattice constant